View metadata, citation and similar papers at core.ac.uk

brought to you by CORE

provided by Elsevier - Publisher Connector

International Journal of Solids and Structures 46 (2009) 3398–3404

Contents lists available at ScienceDirect

International Journal of Solids and Structures

journal homepage: www.elsevier.com/locate/ijsolstr

Adhesive behavior of two-dimensional power-law graded materials

Shaohua Chen [a,*], Cong Yan [a], Aikah Soh [b]

[a] LNM, Institute of Mechanics, Chinese Academy of Sciences, No. 15, BeiSiHuan Xilu, Beijing 100190, China
[b] Department of Mechanical Engineering, The University of Hong Kong, Hong Kong

ARTICLE INFO

Article history:
Received 17 December 2008
Received in revised form 21 April 2009
Available online 18 May 2009

Keywords:
Contact mechanics
Adhesion
Elastic graded materials
JKR model

ABSTRACT

In this paper, we investigate the adhesive contact between a rigid cylinder of radius R and a graded elastic half-space with a Young's modulus varying with depth according to a power-law, $E = E_0(y/c_0)^k$ $(0 < k < 1)$, while the Poisson's ratio v remains constant. The results show that, for a given value of ratio R/c_0, a critical value of k exists at which the pull-off force attains a maximum; for a fixed value of k, the larger the ratio R/c_0, the larger the pull-off force is. For Gibson materials (i.e., $k = 1$ and $v = 0.5$), closed-form analytical solutions can be obtained for the critical contact half-width at pull-off and pull-off force. We further discuss the perfect stick case with both externally normal and tangential loads.

© 2009 Elsevier Ltd. All rights reserved.

1. Introduction

The adhesion system on the feet of geckos has a hierarchical structure (Autumn and Peattie, 2002); the bottom surfaces of the toes of geckos are covered with scalelike structures called lamellae and, each lamella is coated with hundreds of thousands of fibers called setae. Each seta is branched into hundreds of projections called spatulae. The properties of geckos' adhesive system macroscopically appear to be anisotropic and continuously graded with depth. The attachment pad of a cicada shows a smooth top membrane covering an elongated foam structure, which is expected to have a strong elasticity grading (Scherge and Gorb, 2001). Based on an adhesive contact model of anisotropic materials, Chen and Gao (2007) showed that the anisotropic feature could potentially explain the on-the-fly adhesion release of geckos. This leads us to the following question: What is the adhesive behavior of graded materials?

The current studies on contact behavior for graded elastic materials are limited, and while the few existing models are only applicable to certain individual cases and do not consider the effects of adhesion. For example, the models developed by Holl (1940), Hruban (1958), Lekhnitskii (1962) and Booker et al. (1985a,b) are all limited to problems involving a point or line load on a graded elastic half-space, while the models of Gibson (1967), Gibson et al. (1971), Gibson and Sills (1975), Brown and Gibson (1972), Awojobi and Gibson (1973) and Calladine and Greenwood (1978) are limited to a linearly graded elastic strata.

Recent advancements in indentation theory have been valuable in shedding light on the deformation mechanisms of elastic graded materials. For example, Giannakopoulos and Suresh (1997a,b) developed a fundamental understanding of the micromechanics of indentation on a three-dimensional, compositionally graded elastic solid through a combination of analytical, computational and experimental investigations, while Giannakopoulos and Pallot (2000) obtained indentation solutions of a rigid cylinder and a rigid flat punch on elastic graded substrates. A simple framework for the two-dimensional adhesive contact model of graded materials was also given by Giannakopoulos and Pallot (2000), but without any discussion of the adhesion behaviors. Chen et al. (submitted for publication) analyzed the problem of a sphere in adhesive contact with a power-law graded half-space and obtained closed-form analytical solutions of the critical contact radius and the critical force at pull-off.

The present paper is aimed to extend the three-dimensional adhesive contact model (Chen et al., submitted for publication) to a plane strain problem. The adhesion behavior of graded materials will be mainly discussed within the framework of adhesive contact mechanics, which has so far been widely extended (Chaudhury et al., 1996; Johnson and Greenwood, 1997; Greenwood and Johnson, 1998) based on three famous theories (Johnson et al., 1971; Derjaguin et al., 1975; Maugis, 1992). It is hoped that the solutions in the present paper will help researchers understand the adhesion behaviors of graded tissues in biology.

2. Plain strain model with only normal load

A plane strain model of a rigid cylinder of radius R in adhesive contact with an elastic graded half-space is illustrated in Fig. 1. A set of Cartesian coordinates x and y are set up such that x lies along the interface and y points into the depth of the material. An external normal force P is placed on the above cylinder.

* Corresponding author. Tel.: +86 10 82543960; fax: +86 10 82543977.
E-mail address: chenshaohua72@hotmail.com (S. Chen).

0020-7683/$ - see front matter © 2009 Elsevier Ltd. All rights reserved.
doi:10.1016/j.ijsolstr.2009.05.006

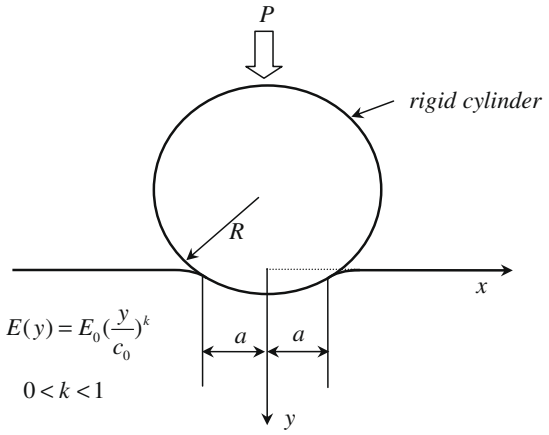

Fig. 1. Schematic of a rigid cylinder of radius R subject to a normal load P in contact with an elastic graded half space with a Young's modulus varying with depth y according to $E(y) = E_0(y/c_0)^k$.

The Young's modulus of the graded half-space varies with depth according to a general power-law

$$E(y) = E_0(y/c_0)^k, \quad 0 < k < 1, \tag{1}$$

where E_0 is a reference modulus, c_0 a characteristic depth of modulus variation, and k the power exponent. The power law variation of the elastic modulus with depth is shown in Fig. 2.

According to Giannakopoulos and Pallot (2000), Green functions describing the relations of the interfacial displacements and tractions in the contact region can be expressed as

$$\frac{\beta c_0^k \sin(\pi\beta/2)}{2(1+k)I_k E^*} \int_{-a}^{a} \frac{p(s)}{k|x-s|^k}\,\mathrm{d}s = \bar{u}_y(x), \quad (-a < x < a), \tag{2}$$

where $p(x)$ denotes the normal traction in the contact region $-a < x < a$. $\bar{u}_y$ denotes the normal interfacial displacement, which can be written as (Johnson, 1985)

$$\bar{u}_y = \delta_y - \frac{x^2}{2R}, \quad (-a < x < a), \tag{3}$$

where δ_y is the vertical translation of the rigid cylinder, and $x^2/2R$ comes from the parabolic assumption for the surface profile of the rigid cylinder (Johnson, 1985).

The other parameters in Eq. (2) are given by

$$\begin{cases} I_k = \frac{\pi\Gamma(3+k)}{2^{k+2}(2+k)\Gamma\left(\frac{3+k+\beta}{2}\right)\Gamma\left(\frac{3+k-\beta}{2}\right)}, \\ \beta = \sqrt{(1+k)\left(1-\frac{kv}{1-v}\right)}, \quad E^* = \frac{E_0}{1-v^2} \end{cases}, \tag{4}$$

while Γ is the Gamma function, and v is the Poisson's ratio of the graded half-space.

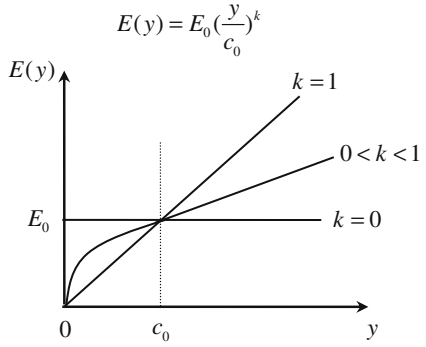

Fig. 2. The power law variation of the elastic modulus $E(y)$ with depth y.

Following Johnson (1985) and Maugis (1992), the adhesive contact pressure $p(x)$ can be decomposed into two normal tractions, $p_1(x)$ and $p_2(x)$,

$$p(x) = p_1(x) - p_2(x), \tag{5}$$

where $p_1(x)$ denotes the indentation pressure between a rigid cylindrical punch and a graded half-space, and $p_2(x)$ is the indentation pressure between a flat punch and a graded half-space.

The total external force P corresponding to the adhesive pressure $p(x)$ can also be decomposed into two parts as

$$P = P_1 - P_2, \quad \int_{-a}^{a} p_1(x)\,\mathrm{d}x = P_1, \quad \int_{-a}^{a} p_2(x)\,\mathrm{d}x = P_2, \tag{6}$$

where P_1 and P_2 are the normal forces associated with the pressures $p_1(x)$ and $p_2(x)$, which have been given by Giannakopoulos and Pallot (2000) in the indentation problems as

$$p_1(x) = f_1(k)\frac{P_1}{2a}\left[1-\left(\frac{x}{a}\right)^2\right]^{\frac{1+k}{2}}, \quad p_2(x) = f_2(k)\frac{P_2}{a}\left[1-\left(\frac{x}{a}\right)^2\right]^{\frac{k-1}{2}}, \tag{7}$$

with functions $f_1(k)$ and $f_2(k)$

$$f_1(k) = \frac{\Gamma(3+k)}{2^{(1+k)}\Gamma^2\left(\frac{3+k}{2}\right)}, \quad f_2(k) = \frac{\Gamma(1+k)}{2^k\Gamma^2\left(\frac{1+k}{2}\right)}, \tag{8}$$

and

$$P_1 = a^{2+k}\frac{E^*}{c_0^k}\frac{\pi}{4R}f_3(k,\beta), \quad P_2 = \frac{\pi E^* a^k \delta_{y2}}{2\bar{h}c_0^k}, \tag{9}$$

$$\begin{cases} f_3(k,\beta) = \frac{2(1+k)^2}{\beta(k+2)\sin(\beta\pi/2)}\frac{\Gamma\left(\frac{1+k}{2}\right)}{\Gamma\left(\frac{3+k+\beta}{2}\right)\Gamma\left(\frac{3+k-\beta}{2}\right)\Gamma\left(\frac{1-k}{2}\right)}, \\ \bar{h}(k,v) = \frac{2}{k(k+2)f_3(k,\beta)}, \end{cases} \tag{10}$$

in which δ_{y2} denotes the normal displacement of the flat punch given in Eq. (13) in the following text.

Substituting Eq. (7) into Eq. (5) yields the adhesive contact pressure

$$p(x) = f_1(k)\frac{P_1}{2a}\left[1-\left(\frac{x}{a}\right)^2\right]^{\frac{1+k}{2}} - f_2(k)\frac{P_2}{a}\left[1-\left(\frac{x}{a}\right)^2\right]^{\frac{k-1}{2}}, \quad 0 < k < 1. \tag{11}$$

The above equation shows that the singularity of the normal traction in the contact region is $(k-1)/2$. Compared to the singularity of $-1/2$ in the classical JKR model, the conclusion can be drawn that the interface cracking in the adhesive contact model for power-law graded materials is suppressed.

The translation δ_y in the present adhesive contact model can also be decomposed into two parts: δ_{y1}, corresponding to the indentation case with a cylindrical punch, and δ_{y2}, corresponding to the case with a flat punch (Giannakopoulos and Pallot, 2000), i.e.,

$$\delta_y = \delta_{y1} - \delta_{y2}, \quad 0 < k < 1 \tag{12}$$

and

$$\delta_{y1} = \frac{a^2}{2Rk}, \quad \delta_{y2} = \bar{h}(k,v)\frac{c_0^k}{E^*}\frac{2P_2}{\pi a^k}. \tag{13}$$

Substituting Eqs. (3), (11) and (12) into the following expression for the total elastic strain energy stored in the power-law graded half space,

$$U_E = \frac{1}{2}\int_{-a}^{a} p(x)\bar{u}_y(x)\,\mathrm{d}x = \int_0^a p(x)\bar{u}_y(x)\,\mathrm{d}x, \tag{14}$$

and utilizing the definition of the Gamma function Γ, we obtain

$$U_E = \frac{\delta_y}{2}(P_1 - P_2) - f_1(k)\frac{P_1 a^2\sqrt{\pi}}{16R}\frac{\Gamma\left(\frac{3+k}{2}\right)}{\Gamma\left(3+\frac{k}{2}\right)} + f_2(k)\frac{P_2 a^2\sqrt{\pi}}{8R}\frac{\Gamma\left(\frac{1+k}{2}\right)}{\Gamma\left(2+\frac{k}{2}\right)}. \tag{15}$$

Assuming no energy is dissipated in the adhesion process, the surface energy U_s in this plane strain model can be expressed as

$$U_s = -2a\Delta\gamma, \tag{16}$$

where $\Delta\gamma$ is the work of adhesion.

The total energy, which is the sum of the elastic strain energy and the surface energy, can be written as

$$U_T = U_E + U_S. \tag{17}$$

Equilibrium can be achieved when

$$\left.\frac{\partial U_T}{\partial a}\right|_{\delta_y} = 0 \tag{18}$$

for a desired δ_y.

Substituting Eqs. (15)–(17) into Eq. (18) yields

$$2\Delta\gamma = \frac{\delta_y}{2}\left(\left.\frac{\partial P_1}{\partial a}\right|_{\delta_y} - \left.\frac{\partial P_2}{\partial a}\right|_{\delta_y}\right) - f_1(k)\frac{\sqrt{\pi}}{16R}\frac{\Gamma\left(\frac{3+k}{2}\right)}{\Gamma\left(3+\frac{k}{2}\right)}\left(2aP_1 + a^2\left.\frac{\partial P_1}{\partial a}\right|_{\delta_y}\right) + f_2(k)\frac{\sqrt{\pi}}{8R}\frac{\Gamma\left(\frac{1+k}{2}\right)}{\Gamma\left(2+\frac{k}{2}\right)}\left(2aP_2 + a^2\left.\frac{\partial P_2}{\partial a}\right|_{\delta_y}\right), \tag{19}$$

where we have

$$\frac{\partial P_1}{\partial a} = \frac{E^*}{c_0^k}\frac{\pi f_3(k,\beta)(2+k)a^{1+k}}{4R},$$
$$\frac{\partial P_2}{\partial a} = \frac{(k+2)E^*\pi a^{k+1}}{4c_0^k\bar{h}(k,\nu)Rk} - \frac{kE^*\pi a^{k-1}\delta_y}{2c_0^k\bar{h}(k,\nu)}. \tag{20}$$

Substituting Eqs. (9), (12) and (20) into (19) yields

$$\frac{\bar{h}k}{\pi}\left(\frac{a}{R}\right)^{-(k+1)}(\alpha)^{-k}\left(\frac{\Delta\gamma}{E^*R}\right)\left(\frac{P}{\Delta\gamma}\right)^2 - \frac{1}{2}\left[f_3\bar{h}\left(\frac{3k}{2}+1\right) - \frac{1}{k}\right]\frac{a}{R}\frac{P}{\Delta\gamma} + \left[\frac{\pi f_3^2\bar{h}(k+1)}{8} - \frac{\pi}{4k^2\bar{h}(k+2)}\right]\left(\frac{a}{R}\right)^{k+3}(\alpha)^k\frac{E^*R}{\Delta\gamma} - 2 = 0, \quad 0<k<1, \tag{21}$$

which establishes the relation between the normalized external force $P/\Delta\gamma$ and the normalized contact half-width a/R as a function of parameters k, $\Delta\gamma/(E^*R)$, β and α, where α is called modulus variation rate,

$$\alpha = \frac{R}{c_0}. \tag{22}$$

For a determined radius R, the larger the value of c_0, the smaller the modulus variation rate α will be.

In contrast to the three-dimensional case (Chen et al., submitted for publication), simple closed-form solutions to Eq. (21) cannot be obtained easily. Numerical calculation must be carried out to analyze the interfacial adhesion behavior. However, it can be easily solved for a special case, i.e., a Gibson solid.

In the case of a Gibson half-space, we have

$$k = 1 \quad \text{and} \quad \nu = 0.5. \tag{23}$$

Eq. (21) can be simplified as

$$\frac{3P^2c_0}{8a^2E_0} - \frac{aP}{3R} + \frac{2a^4E_0}{27R^2c_0} - 2\Delta\gamma = 0, \tag{24}$$

which yields an explicit solution,

$$P = \frac{4a^3E_0}{9Rc_0} - 4a\sqrt{\frac{\Delta\gamma E_0}{3c_0}}. \tag{25}$$

Then, the critical contact half-width a_{cr} at pull-off can be obtained as

$$a_{cr} = \left(\frac{3R^2\Delta\gamma c_0}{E_0}\right)^{\frac{1}{4}}, \tag{26}$$

and the pull-off force P_{cr} is

$$P_{cr} = -\frac{8}{3}\left(\frac{R^2E_0\Delta\gamma^3}{3c_0}\right)^{\frac{1}{4}}. \tag{27}$$

3. Plane strain model with both normal and tangential loads

The non-slipping model is considered in this section, as shown in Fig. 3. The rigid cylinder is first subjected to a normal load P and then a tangential force Q. The contact region is assumed to be asymmetric with right and left contact lengths a and b, which will be later found to be equal. In addition, the normal contact tractions are not affected by the tangential force due to the negligible effect (Johnson, 1985), and the tangential load is assumed to be properly added without introducing any moments at the contact interface. Thus, according to Giannakopoulos and Pallot (2000), the normal and tangential tractions, $p(x)$ and $q(x)$, satisfy the following formula:

$$\begin{cases} \frac{c_0^k}{E^*}\frac{k+1}{\beta}\frac{\sin(\beta\pi/2)}{2I_k}\int_{-b}^{a}\frac{q(x)}{k|x-s|^k} = \delta_x = \text{const.}, \\ \frac{\beta c_0^k\sin(\pi\beta/2)}{2(1+k)I_kE^*}\int_{-b}^{a}\frac{p(s)}{k|x-s|^k}\,\mathrm{d}s = \bar{u}_y(x) = \delta_y - \frac{x^2}{2R}, \end{cases} \quad -b \leqslant x \leqslant a,\ 0<k<1. \tag{28}$$

The adhesive normal traction, after solving the second equation of (28), can be obtained as

$$p(x) = p_1(x) - p_2(x), \quad -b < x < a, \tag{29}$$

where

$$p_1(x) = \frac{P_1}{a+b}\frac{\Gamma(3+k)}{2^{1+k}\Gamma^2\left(\frac{3+k}{2}\right)}\left[\frac{4ab}{(a+b)^2}\right]^{\frac{1+k}{2}}\left[\left(1-\frac{x}{a}\right)\left(1+\frac{x}{b}\right)\right]^{\frac{1+k}{2}}, \tag{30}$$

$$p_2(x) = \frac{P_2}{2^k}\frac{2}{a+b}\left[\frac{(a+b)^2}{4ab}\right]^{\frac{1-k}{2}}\frac{\Gamma(1+k)}{\Gamma^2\left(\frac{1+k}{2}\right)}\left[\left(1-\frac{x}{a}\right)\left(1+\frac{x}{b}\right)\right]^{\frac{k-1}{2}}. \tag{31}$$

In nature, P_1 is the load due to the cylindrical punch stress distribution, and P_2 is the load due to the flat punch solution, i.e.,

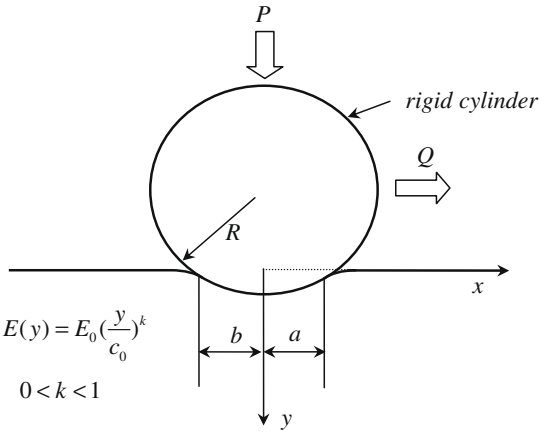

Fig. 3. Schematic of a rigid cylinder of radius R, subject to a tangential force Q after a normal force P, in contact with an elastic graded half space with a Young's modulus varying with depth y as $E(y) = E_0(y/c_0)^k$, where $0 < k < 1$. The right and left contact lengths are a and b, respectively.

$$\int_{-b}^{a} p_1(x)\,dx = P_1,\ \int_{-b}^{a} p_2(x)\,dx = P_2, \tag{32}$$

The total load P in the adhesive model can be obtained as $P = P_1 - P_2$.

The corresponding total depth, δ_y, can also be expressed in the same manner as Eq. (12), while

$$\delta_{y1} = \frac{4a^2 + (k-1)(a-b)^2}{8Rk} \tag{33}$$

and

$$\delta_{y2} = \frac{c_0^k}{E^*}\frac{2^{k+1}P_2}{\pi(a+b)^k}\bar{h}(k,v). \tag{34}$$

The relation between the load P_1 and the contact lengths a and b is found from the second equation of (28),

$$P_1 = \frac{\pi E^*(a+b)^k[4a^2-(a-b)^2]}{2^{k+4}c_0^k R} f_3(k,\beta). \tag{35}$$

Now, focusing on the effect of the tangential force, we can obtain the tangential traction in the contact region from the first equation of (28) as

$$q(x) = \frac{2Q}{(a+b)}\left[\frac{(a+b)^2}{4ab}\right]^{\frac{1-k}{2}}\left[\left(1-\frac{x}{a}\right)\left(1+\frac{x}{b}\right)\right]^{\frac{k-1}{2}} f_2(k), \quad -b < x < a \tag{36}$$

and the relative tangential displacement δ_x in the form,

$$\delta_x = \frac{2^{k+1}c_0^k Q}{\pi E^*(a+b)^k}\bar{\delta}, \tag{37}$$

where

$$\bar{\delta} = \frac{\sin(\beta\pi/2)\Gamma\left(\frac{1-k}{2}\right)}{k\beta\Gamma\left(\frac{1+k}{2}\right)}\Gamma\left(\frac{3+k+\beta}{2}\right)\Gamma\left(\frac{3+k-\beta}{2}\right). \tag{38}$$

The total elastic strain energy stored in the power-law graded half space is

$$\begin{aligned} U_E(a,b) &= U_{Ep}(a,b) + U_{Eq}(a,b) \\ &= \frac{1}{2}\int_{-b}^{a} p(x)\bar{u}_y(x)\,dx + \frac{1}{2}\int_{-b}^{a} q(x)\delta_x\,dx. \end{aligned} \tag{39}$$

Assuming there is no energy dissipation in the adhesion process, the surface energy U_s is linked to the work of adhesion, $\Delta\gamma$, by

$$U_s = -(a+b)\Delta\gamma. \tag{40}$$

Then, equilibrium can be achieved when

$$\left.\frac{\partial U_T(a,b)}{\partial a}\right|_{\delta_y,\delta_x} = \left.\frac{\partial U_T(a,b)}{\partial b}\right|_{\delta_y,\delta_x} = 0, \tag{41}$$

for a desired δ_y due to the normal loading and δ_x due to the tangential loading, where U_T is the total energy as expressed in Eq. (17).

Eq. (41) leads to

$$a = b. \tag{42}$$

The above identity can also be obtained from a simple analysis: for the case with tangential traction alone, the energy release rates should be identical at both contact edges (similar to an external interface crack problem), both of which are equal to the work of adhesion $\Delta\gamma$ at equilibrium from the fracture mechanics point of view. Then, we can find that $a = b$. The same result should be obtained for the case with the normal traction alone. In the present model, due to the uncoupling effects of the normal and tangential tractions, the neglect of effects of any moments at the contact interface, $a = b$, should be satisfied.

Thus, the normal traction $p(x)$ and the relation between the normal loading P and the contact half-width a are simplified as the counterparts in Section 3. The tangential traction $q(x)$ in Eq. (36) is also reduced to

$$q(x) = f_2(k)\frac{Q}{a}\left[1-\left(\frac{x}{a}\right)^2\right]^{\frac{k-1}{2}}, \tag{43}$$

and the relative tangential displacement δ_x in Eq. (37) becomes

$$\delta_x = \frac{c_0^k}{E^*}\frac{2Q}{\pi a^k}\bar{\delta}. \tag{44}$$

The elastic strain energy produced by the tangential traction alone can be obtained as

$$U_{E_q} = \frac{1}{2}\int_{-a}^{a} q(x)\delta_x\,dx = \frac{1}{2}Q\delta_x \tag{45}$$

and

$$\left.\frac{\partial U_{E_q}}{\partial a}\right|_{\delta_x} = \frac{\Gamma(1+k)k\bar{\delta}Q^2c_0^k}{2^k\Gamma\left(\frac{1+k}{2}\right)\Gamma\left(1+\frac{k}{2}\right)\sqrt{\pi}E^*}a^{-(k+1)} \tag{46}$$

for a desired δ_x.

At equilibrium of the adhesive system, it is required that

$$\left.\frac{\partial U_T}{\partial a}\right|_{\delta_y,\delta_x} = \left.\frac{\partial U_{Ep}}{\partial a}\right|_{\delta_y} + \left.\frac{\partial U_{Eq}}{\partial a}\right|_{\delta_x} - 2\Delta\gamma = 0 \tag{47}$$

for desired δ_y, δ_x.

It is straightforward, if one follows the same procedure outlined in Section 2, to obtain the following relation:

$$\begin{aligned} &\left[\frac{\bar{h}k\sin^2\theta}{\pi} + \frac{k\bar{\delta}\cos^2\theta}{\pi}\right]\left(\frac{a}{R}\right)^{-(k+1)}(\alpha)^{-k}\left(\frac{\Delta\gamma}{E^*R}\right)\left(\frac{F}{\Delta\gamma}\right)^2 \\ &\quad - \frac{1}{2}\left[f_3\bar{h}\left(\frac{3k}{2}+1\right) - \frac{1}{k}\right]\frac{a}{R}\frac{F\sin\theta}{\Delta\gamma} \\ &\quad + \left[\frac{\pi f_3^2\bar{h}(k+1)}{8} - \frac{\pi}{4k^2\bar{h}(k+2)}\right]\left(\frac{a}{R}\right)^{k+3}(\alpha)^k\frac{E^*R}{\Delta\gamma} - 2 = 0, \end{aligned} \tag{48}$$

The above equation gives the apparent resultant force F as a function of the apparent pulling angle θ, where

$$F = \sqrt{P^2+Q^2}, \quad \theta = \arcsin(P/F). \tag{49}$$

Numerical analysis for Eq. (48) will be used to find the effects of the apparent angle θ on the pull-off process, which is given in the following section.

4. Numerical analysis

A numerical method is used in this section to solve the governing equations (21) and (48). Our interest is focused on the adhesion behavior of the power-law graded material; the effects of the gradient exponent k, the modulus variation rate α and the apparent pulling angle θ on the pull-off force and the critical contact width at pull-off.

4.1. Plane strain model under a normal force

We first study the effects of the gradient exponent k and the modulus variation rate α for the plane strain model under a normal force. The relation between the normalized contact width a/R and the dimensionless normal force $P/\Delta\gamma$ is shown in Fig. 4 for different values of k and α, while the other parameters of the system are

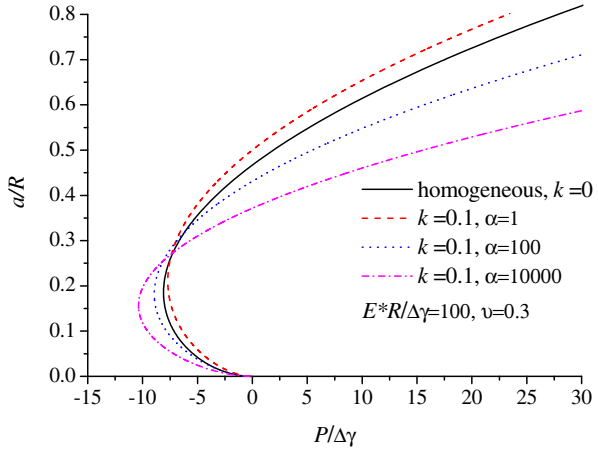

Fig. 4. Plot of the normalized external normal force $P/\Delta\gamma$ as a function of the normalized contact half-width a/R with given parameters $E^*R/\Delta\gamma = 100$, $v = 0.3$, $k = 0.1$ and different values of α for the model in Fig. 1. The result for $k = 0$ corresponds to the two-dimensional classical JKR solution.

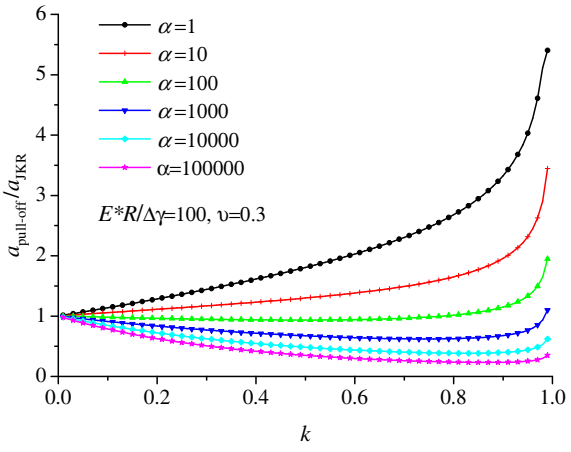

Fig. 6. Effects of the exponent k on the normalized pull-off contact width $a_{\text{pull-off}}/a_{\text{JKR}}$ with given parameters $E^*R/\Delta\gamma = 100$, $v = 0.3$ and different values of α for the model in Fig. 1.

constant. For comparison purposes, the corresponding plane strain JKR solution (Chaudhury et al., 1996) when $k = 0$ is also included in Fig. 4.

The effects of the gradient exponent k and the modulus variation rate α on the pull-off force, *i.e.*, the critical force needed to separate the contact, are shown in Fig. 5. Apparently, both parameters can affect the pull-off force significantly. For the prescribed values of $E^*R/\Delta\gamma$ and v, the pull-off force seems to decrease monotonically with an increase in the gradient exponent k for small or moderate values of α (e.g., $\alpha = 1$). For large values of α, the pull-off force increases initially with k, reaches a maximum value and then decreases with further increase in k. For a given value of k, the pull-off force increases with α monotonically.

The critical contact width at pull-off is also influenced by k and α, as shown in Fig. 6, where it can be observed that the variation trend of the critical contact width is opposite to that of the pull-off force. For large values of α, the critical contact width decreases initially with k, reaches a minimum value and then increases with further increase in k. For small or moderate values of α (e.g. $\alpha = 1$), the critical contact width increases with k monotonically. For a given value of k, the critical contact width decreases with α monotonically.

The effects of $E^*R/\Delta\gamma$ on the pull-off force are shown in Fig. 7. It is observed that $E^*R/\Delta\gamma$ does not show a significant effect on the pull-off force, especially for small or moderate values of α.

4.2. Plane strain model under both normal and tangential loads

The results for the plane strain contact model under both normal and tangential loads are discussed in this section.

Fig. 8(a)–(d) shows the normalized pull-off force $F_{\text{pull-off}}/F_{\text{JKR}}$ as functions of the apparent pulling angle θ for different values of the gradient exponent k and of the gradient variation rate α when $E^*R/\Delta\gamma$ is set. It is observed that the pull-off force is affected significantly by θ, k and α. For large values of α, the homogeneous case ($k = 0$) seems to yield generally smaller pull-off forces compared to the graded cases; for small or moderate values of α, the homogeneous case can give pull-off forces higher than the graded cases. For a given value of α, there also exists a critical value of k, beyond which the elastic graded materials may actually give lower pull-off forces than the homogenous case. For a sufficiently small value of α, no elastic graded material provides better adhesion than the homogeneous material.

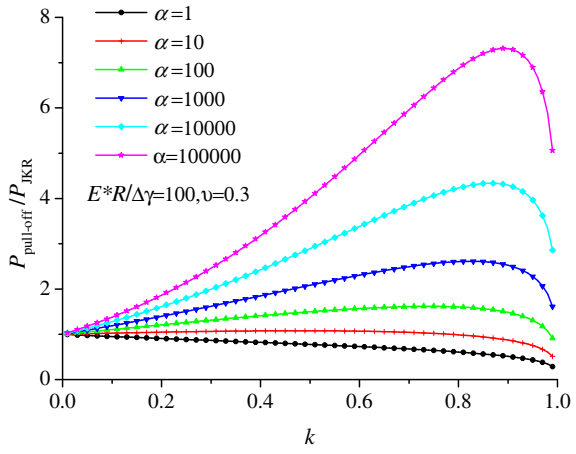

Fig. 5. Effects of exponent k on the normalized pull-off force $P_{\text{pull-off}}/P_{\text{JKR}}$ with given parameters $E^*R/\Delta\gamma = 100$, $v = 0.3$ and different values of α for the model in Fig. 1.

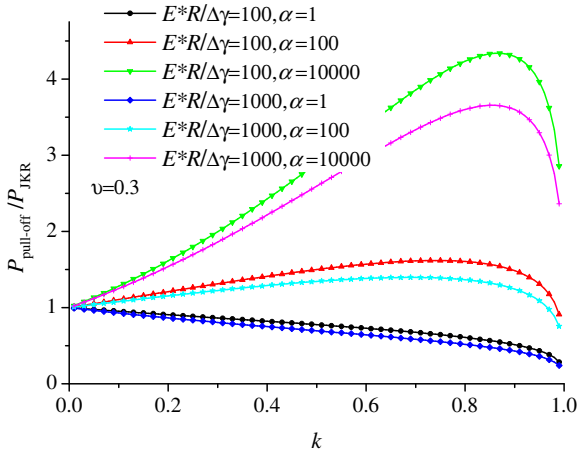

Fig. 7. Effects of different values $E^*R/\Delta\gamma$ on the relationship between the normalized pull-off force $P_{\text{pull-off}}/P_{\text{JKR}}$ and the exponent k with a Poisson's ratio $v = 0.3$ and a set of given values α for the model in Fig. 1.

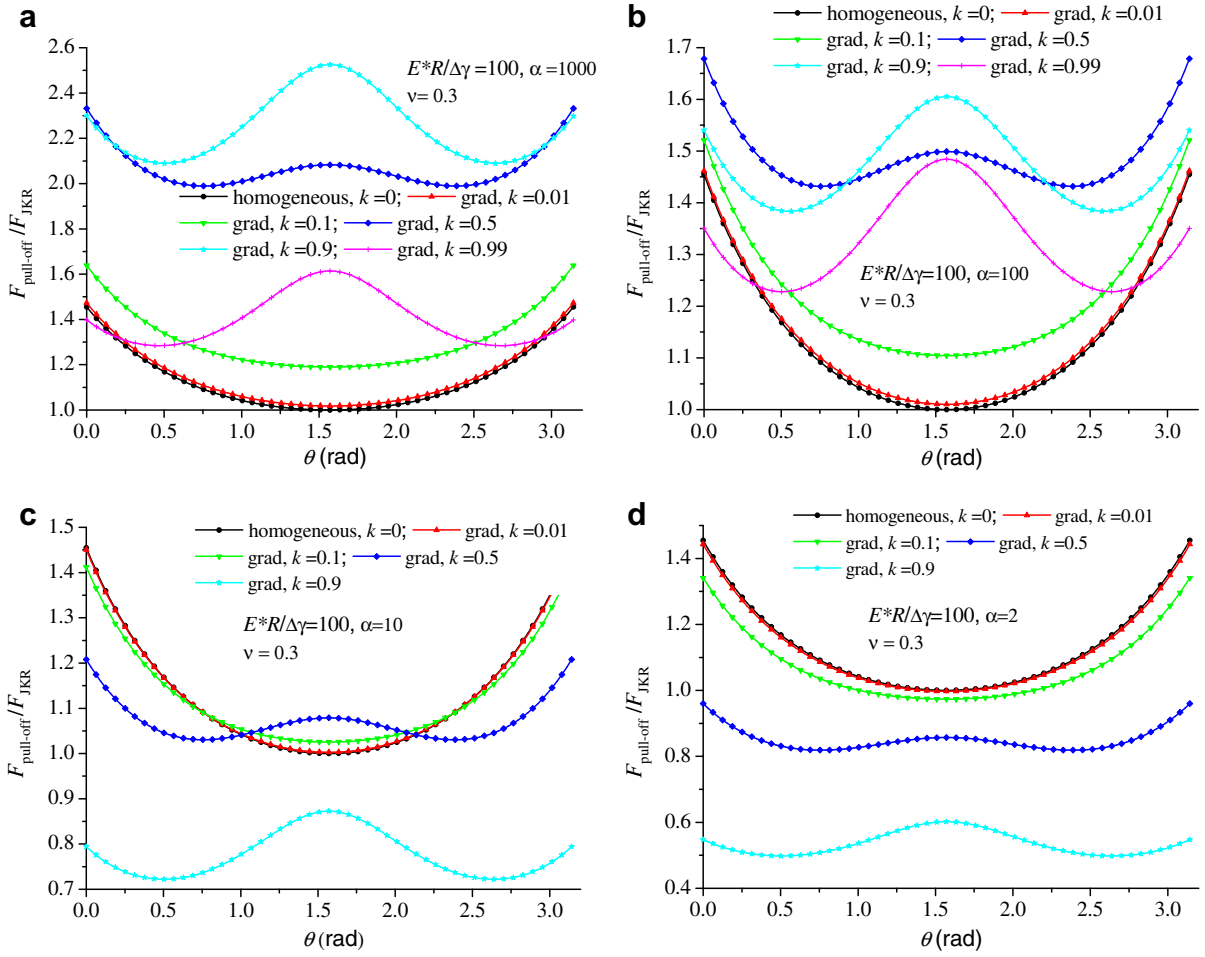

Fig. 8. Plots of normalized pull-off force $F_{\text{pull-off}}/F_{\text{JKR}}$ as a function of the apparent pulling angle θ with given parameters $E^*R/\Delta\gamma$ and different values of the exponent k for the model in Fig. 3. F_{JKR} is the pull-off force of the classical two-dimensional JKR model, in which $k = 0$ and $\theta = \pi/2$. (a) $\alpha = 1000$, (b) $\alpha = 100$, (c) $\alpha = 10$ and (d) $\alpha = 2$, where $\alpha = R/c_0$.

5. Summary

The present paper has aimed to develop adhesive contact models for general power-law graded materials and to compare the adhesion behavior of these materials to that of homogeneous isotropic materials. The analysis indicates that there exists a critical gradient exponent k, at which the pull-off force exhibits a maximum value. The gradient variation rate controls the magnitude of the pull-off force: for an elastic graded material with a larger value of α, the pull-off force is larger than that for the corresponding isotropic material. If the value of α is smaller, the pull-off force for the graded material is smaller than that for the corresponding isotropic case.

Closed-form analytical solutions for the critical contact area and the critical force at pull-off were obtained for the limit case, a Gibson material.

In the case with both normal and tangential loads, the pull-off force is mainly controlled by the values of the gradient exponent k, the gradient variation rate α and the apparent pulling angle θ.

The finding in the present paper that gradient elasticity leads to gradient-sensing adhesion provides one possible way to understand the elasticity gradient in some biological adhesive tissues and provides a rational assessment of the possible advantages and disadvantages of graded surfaces in tribological applications.

Acknowledgments

The work reported here is supported by the National Nature Science Foundation of China through Grants #10672165, #10732050, and #10721202, and the key project of Chinese Academy of Sciences through Grant KJCX2-YW-M04 and CAS Innovation Program.

References

Autumn, K., Peattie, A.M., 2002. Mechanisms of adhesion in geckos. Integr. Compar. Biol. 42, 1081–1090.
Awojobi, A.O., Gibson, R.E., 1973. Plane strain and axially symmetric problems of a linearly nonhomogeneous elastic half-space. Q. J. Mech. Appl. Math. 26, 285–302.
Booker, J.R., Balaam, N.P., Davis, E.H., 1985a. The behavior of an elastic nonhomogeneous half-space. Part I. Line and point loads. Int. J. Numer. Anal. Methods Geomech. 9, 353–367.
Booker, J.R., Balaam, N.P., Davis, E.H., 1985b. The behavior of an elastic nonhomogeneous half-space. Part II. Circular and strip footings. Int. J. Numer. Anal. Methods Geomech. 9, 369–381.
Brown, P.T., Gibson, R.E., 1972. Surface settlement of a deep elastic stratum whose modulus increases linearly with depth. Can. Geotech. J. 9, 467–476.
Calladine, C.R., Greenwood, J.a., 1978. Line and point loads on a non-homogeneous incompressible elastic half-space. Q. J. Appl. Match. 28, 507–529.
Chaudhury, M.K., Weaver, T., Hui, C.Y., Kramer, E.J., 1996. Adhesion contact of cylindrical lens and a flat sheet. J. Appl. Phys. 80, 30–37.
Chen, S., Gao, H., 2007. Bio-inspired mechanics of reversible adhesion: orientation-dependent adhesion strength for non-slipping adhesive contact with transversely isotropic elastic materials. J. Mech. Phys. Solids 55, 1001–1015.
Chen, S., Yan, C., Zhang, P., Gao, H., submitted for publication. Adhesive contact on graded materials.

Derjaguin, B.V., Muller, V.M., Toporov, Y.P., 1975. Effect of contact deformations on the adhesion of particles. J. Colloid Interface Sci. 53, 314–326.
Giannakopoulos, A.E., Pallot, P., 2000. Two-dimensional contact analysis of elastic graded materials. J. Mech. Phys. Solids 48, 1597–1631.
Giannakopoulos, A.E., Suresh, S., 1997a. Indentation of solids with gradients in elastic properties: part I. Point force. Int. J. Solids Struct. 34, 2357–2392.
Giannakopoulos, A.E., Suresh, S., 1997b. Indentation of solids with gradients in elastic properties: part II. Axisymmetric indenters. Int. J. Solids Struct. 34, 2393–2428.
Gibson, R.E., 1967. Some results concerning displacements and stresses in a non-homogeneous elastic half-space. Geotechnique 17, 58–67.
Gibson, R.E., Sills, G.C., 1975. Settlement of a trip load on a non-homogeneous orthotropic incompressible elastic half-space. Q. J. Mech. Appl. Math. 28, 233–243.
Gibson, R.E., Brown, P.T., Andrew, K.R.F., 1971. Some results concerning displacements in a non-homogeneous elastic layer. ZAMP 22, 855–864.
Greenwood, J.A., Johnson, K.L., 1998. An alterative to the Maugis model of adhesion between elastic spheres. J. Phys. D 31, 3279–3290.
Holl, D.L., 1940. Stress transmission in earths. In: Proceedings of the High Research Board, vol. 20, pp. 709–721.
Hruban, K., 1958. The basic problem of a non-linear and non-homogeneous half-space. In: Non-homogeneity in Elasticity and Plasticity IUTAM Symposium. Pergamon Press, Warsaw, pp. 53–61.
Johnson, K.L., 1985. Contact Mechanics. Cambridge University Press, Cambridge.
Johnson, K.L., Greenwood, J.A., 1997. An adhesion map for the contact of elastic spheres. J. Colloid Interface Sci. 192, 326–333.
Johnson, K.L., Kendall, K., Roberts, A.D., 1971. Surface energy and the contact of elastic solids. Proc. Roy. Soc. Lond. A 324, 301–313.
Lekhnitskii, S.G., 1962. Radial distribution of stresses in a wedge and in a half-plane with variable modulus of elasticity. PMM 26, 146–151.
Maugis, D., 1992. Adhesion of spheres: the JKR-DMT transition using a Dugdale model. J. Colloid Interface Sci. 150, 243–269.
Scherge, M., Gorb, S., 2001. Biological Micro- and Nano-Tribology – Nature's Solutions. Springer, Berlin.